Functional Materials Letters
Vol. 10, No. 1 (2017) 1740006 (8 pages)

DOI: 10.1142/S1793604717400069

World Scientific
www.worldscientific.com

A short review on the interaction of precipitates and martensitic transitions in CuZnAl shape memory alloys

Franco de Castro Bubani
Centro Atómico Bariloche (CNEA) and CONICET
Av. E. Bustillo km. 9,5 (8400) S.C.de Bariloche, Argentina
franco@cab.cnea.gov.ar

Francisco Carlos Lovey
Centro Atómico Bariloche (CNEA) and Instituto Balseiro
Universidad Nacional de Cuyo
Av. E. Bustillo km. 9,5 (8400) S.C.de Bariloche, Argentina
lovey@cab.cnea.gov.ar

Marcos Leonel Sade*
Centro Atómico Bariloche (CNEA), CONICET and Instituto Balseiro
Universidad Nacional de Cuyo
Av. E. Bustillo km. 9,5 (8400) S.C.de Bariloche, Argentina
sade@cab.cnea.gov.ar, marcossade05@yahoo.com.ar

Received 30 November 2016; Accepted 23 December 2016; Published 2 February 2017

The main effects of γ non-equilibrium nanoprecipitates in CuZnAl shape memory alloys are briefly reviewed. Aspects related to the nucleation and growth of precipitates are commented on and their effect on stress induced martensitic transitions is analyzed. Results concerning the relationship between the size of precipitates and the hysteresis of the stress induced β-18R transition are studied. The improvement of the two-way shape-memory effect after the introduction of precipitates is shortly commented on. The 18R–6R transition is also analyzed and recent findings on the optimization of the mechanical reversibility associated to the 18R–6R transformation in a matrix with a high density of nano precipitates are reviewed.

Keywords: Shape-memory alloys; precipitation; CuZnAl; Cu base alloys.

1. Introduction

Shape memory alloys (SMAs) have the capacity to return to a predefined shape when the temperature increases sufficiently. The shape-memory effect is caused by martensitic transitions between a metastable parent phase, usually called austenite, and a martensitic phase that can be either thermally or mechanically induced.[1–3]

Some SMAs also present pseudoelasticity, which occurs at a temperature above the beginning of the thermally induced martensitic transition: the austenite transforms into martensite when an external mechanical load is applied, changing the shape of the alloy. When the external load is removed, the martensite retransforms to austenite, and the original shape is recovered. Recoverable pseudoelastic strains greater than 10% in single crystals have been reported[4–6] and, when two sequential martensitic transitions are present, recoverable strains of about 20% are possible.[7–10]

SMAs are often used when they are able to meet specific requirements that outweigh the higher costs associated to these alloys: examples can be found in medicine, dentistry, aerospace engineering, and non-conventional mechanical damping devices and actuators.

Cu-based SMAs are not biocompatible, so possible uses in medicine are restricted to devices placed outside the human body. Nevertheless, Cu-based SMAs and other SMAs with pseudoelastic behavior can be effectively used as dampers of mechanical vibrations, e.g., as non-conventional seismic damping systems in buildings and industrial structures.[11–15]

The mechanical properties of SMAs can be optimized either by controlled modifications of their chemical composition or by thermomechanical treatments. The former often

*Corresponding author.

leads to the discovery of new alloys, whereas the latter may result in new processing and/or training methods. In SMAs, precipitates are usually formed above room temperature, during specific thermal treatments, or during slow cooling. As the mechanical properties of SMAs depend on the size and distribution of precipitates, thermomechanical treatments are an effective method to optimize the properties of SMAs.

The effect of precipitates on SMAs can be described as impressive. However, the specific effects of the introduction of second phase particles depend strongly on the metallic system considered. In NiTi SMAs, the shape-memory effect is very sensitive to the microstructure of the alloy and is normally associated to a two-step transformation from the parent β phase to the R-phase and then to the B19' phase.[16] Different phases can be present in NiTi SMAs, depending on the chemical composition and thermomechanical processing,[16] but precipitation of Ni_4Ti_3, in particular, has a critical effect on the martensitic transition temperatures and path, due to the elastic strain and chemical composition shift around the precipitates.[17,18]

Interesting examples in Fe-based SMAs have been reported: (a) the introduction of NbC precipitates in FeMnSi alloys improves the shape memory effect and the recovery stress during the thermally induced hcp-fcc transformation[19]; (b) the introduction of coherent nanoprecipitates in FeMnAlNi alloys leads to a thermoelastic bevahior associated to a bcc-fcc martensitic transition, a remarkable finding which gave rise to pseudoelasticity in this system[20] and (c) a strong effect on the fcc-bct martensitic transformation was also reported for FeNiCo-based alloys after the introduction of $L1_2$ (γ') precipitates, where the mentioned transition changed its character from non-thermoelastic to thermoelastic.[21] This change also leads to excellent pseudoelastic properties, reported in FeNiCoAlTa.[21] The pseudoelastic properties of Co-based alloys are significantly improved by the introduction of γ' precipitates as reported by Kireeva *et al.* for $Co_{49}Ni_{21}Ga_{30}$ single crystals.[22]

Cu-based alloys are a different case, as specific compositions of CuAlBe, CuAlNi, CuZnAl, CuAlMn, and Cu-based alloys with a higher number of elements show a reasonable behavior concerning shape memory effect and pseudoelasticity without the need to introduce second phases in the system. In fact, CuZnAl, CuAlBe, and CuAlNi alloys are excellent examples of SMAs and have been studied for several years because of their characteristic properties such as one-way shape memory effect, pseudoelasticity, two-way shape memory effect (TWSME) and the rubber effect.[4,7,8,23–29]

These properties are related to the martensitic phase transformations that occur in these systems, which have received much attention indeed. The main martensitic transitions in these alloys are the β-18R and β-2H transformations, where the β phase is a cubic structure which is stable at high temperatures and can be retained at room temperature after quenching. Details on this phase and martensitic structures can be found in Ref. 30.

The specific composition of the alloy determines which of those transitions will take place. Relative phase stabilities, the mechanical properties of the phases involved, methods to control microstructure, stabilization of martensite and ordering reactions have been analyzed in detail.[4,31,32] Single crystals and polycrystalline material have been studied.

Although shape memory properties have been found without introducing second phases in the austenite, it is clear that precipitates might improve specific behaviors, and could also help to control properties like hysteresis, reversibility, critical transformation stresses and mechanical properties. As examples, it can be mentioned that, in CuAlNi single crystals, the introduction of precipitates modify the martensitic transformation temperatures.[33,34] Araujo *et al.* reported that precipitates grown by ageing modify the behavior of martensitic transitions, even changing the type of martensite formed.[34] In CuAlBe, precipitates formed during slow cooling also modify the thermoelastic behavior of the alloy.[29] In CuZnAl single crystals with precipitates, mechanical reversibility up to 20% deformation has been reported,[35] with no plastic deformation in any of the phases involved.

Precipitates can have different effects on martensitic transformations: the hardening of one or several phases in each system, the introduction of stress fields and stored elastic energy associated to the strain of precipitates when the martensitic transformation takes place, etc. In some cases, several contributions might coexist, which requires a specific analysis for each system.

In this paper, attention is focused on the interaction between precipitates and martensitic transformations in the CuZnAl system. Although most recent findings are related to the effect of nanoprecipitates on martensite to martensite transformations, we consider it is in the best interest of readers to extend the scope of the manuscript and include the main effects of precipitates on different aspects of the shape memory properties in CuZnAl alloys. This work is focused on reported results obtained with single crystals and γ non-equilibrium nanoprecipitates, although other precipitates are considered in some cases. The effect of these precipitates on the β-18R martensitic transformation will be analyzed, with an emphasis on the stress induced martensitic transformation. The main results concerning the nucleation and growth of non-equilibrium precipitates will be shortly commented on. Precipitation has been shown to have an effect on the TWSME, a topic which is also shortly considered. Finally, the relationship between γ nanoprecipitates and the 18R–6R martensitic transition is analyzed.

2. On the Interaction Between γ Precipitates and the β-18R Martensitic Transformation

The characteristics of the martensitic transformations in Cu–Zn–Al alloys strongly depend on the presence of γ-type precipitates embedded in the austenite.[36–38] In thermally induced martensitic transitions, the Ms temperature decreases. The magnitude of the shift depends on the thermal treatment, which can, in fact, be correlated with the size of the precipitates.[37,38] It has also been shown that retransformation temperatures significantly increase for larger precipitates, leading to a wider thermal hysteresis.[37,38] Moreover, it has been reported that the shape of the thermally induced cycles, measured by different experimental techniques, is modified during cycling. The behavior becomes asymmetric if the transformation to martensite and the reverse transition to austenite are considered.[39,40]

Particularly, different behaviors concerning martensitic transformation temperatures and hysteresis have been explained considering the effect of stored elastic energy, the energy dissipated due to local plastic deformation in the interaction between the martensite plates and precipitates and changes in the matrix composition.[39,40] Pons *et al.* concluded that stability in thermal cycling increases after the introduction of a dense distribution of coherent precipitates (50 nm size).[40] Finally, a thermally induced transformation producing a single variant, single plate transformation in a β matrix with precipitates has led to a decrease of Ms, and a wider hysteresis which decreases after cycling.[41,42] This was explained by the shape change of the matrix cavity containing the precipitate and the dislocations which form around the precipitates once the martensite is formed.

The effect of precipitates on the stress induced martensitic transition deserves particular attention, mainly because many potential alternatives for applications usually involve applied stresses.[43,44] Pseudoelastic properties might be severely modified due to the interaction between small particles and the advancing martensitic plates. The consequences of this interaction cannot be obtained directly from the analysis of thermally induced martensitic transformation. If the temperature decreases below Ms, strain is minimized by the nucleation and growth of different variants among the precipitates. This mechanism is not readily available when strain is to be maximized according to the applied stress.

Matrix single crystals are the simplest systems available to study the interaction between precipitates and the stress induced martensitic transformation.[45] A couple of significant details about the introduced precipitates are mentioned in the following paragraph.

Several papers reported different features concerning the nucleation and growth of γ precipitates.[38,46] Precise information on the thermal treatments required to introduce coherent precipitates, and on the loss of coherency as precipitates grow is found in Ref. 38. It was clearly shown that the growth of these precipitates follows the Ostwald ripening mechanism for precipitates larger than 100 nm approximately (the radius cubed, r^3, is proportional to the time t) and that precipitates keep coherent with the bcc matrix during the early stages of thermal ageing at 673 K. Additional detailed characteristics of the microstructural features of the γ precipitates embedded in the matrix were presented by Pons and Portier in Ref. 46. These authors, also using high resolution microscopy, determined that, after step quenching, γ precipitates keep coherency up to 50 nm and that they are located on the $L2_1$ antiphase boundaries of the β phase. Moreover, after subsequent flash heating up to 670 K, keeping the samples at this temperature for a few seconds, $L2_1$ domains grow as well as the precipitates which remain on their locations on these boundaries. Previous results had already shown that non-equilibrium precipitates formed along B2 antiphase boundaries and also inside the B2 domains.[47]

In the following paragraphs, the interaction between γ precipitates and the β-18R stress induced martensitic transformations will be considered. Single crystals with a composition around Cu-16.7% Al-14.8% Zn (at.%) are considered in this part of the report. The precipitates were produced with the following thermal treatments[38]: solution treatment at 1120 K for 30 min, followed by cooling to 800 K and then quenching into ice water. In this way, cuboidal precipitates with an average size around 10 nm, as observed by transmission electron microscopy, are obtained. The precipitates density was found to be $\delta = 2.5 \pm 1.1 \times 10^{21}$ precip. m^{-3}. Additional ageing at 500 K for different times allowed precipitates to grow. Precipitate sizes of up to 55 nm were obtained. Ageing times are short enough to keep below the beginning of the Ostwald ripening process in order to maintain a constant precipitates density. In this way, precipitates keep coherent with the β matrix in the analyzed range. A sample distribution of coherent precipitates in CuZnAl is shown in Fig. 1.

Typical curves obtained after tensile stressing single crystals are shown in Figs. 2(a) and 2(b). The first cycle is shown in Fig. 2(a) while cycle 14 is presented in Fig. 2(b). Since a single martensite variant is obtained in each cycle the resolved shear stress can be easily obtained for each value of applied tensile stress. In both figures, resolved shear stress is plotted vs. elongation of the sample.

The following aspects are present throughout the cycling procedures and should be emphasized[45]:

(i) The tensile stresses to transform to martensite increase after the introduction of precipitates. A significant slope of the curve is observed during transformation.

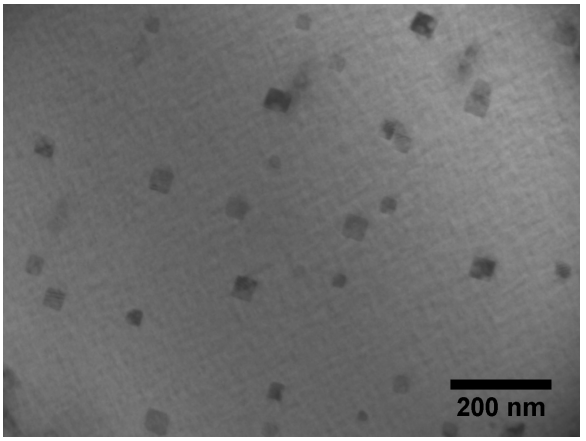

Fig. 1. Coherent nanometric γ precipitates in a CuZnAl single crystal.

(ii) The stresses to transform to martensite strongly decrease after cycling and an asymptotic behavior is reached after around a hundred cycles. The loops in the asymptotic stage show a noticeable slope.

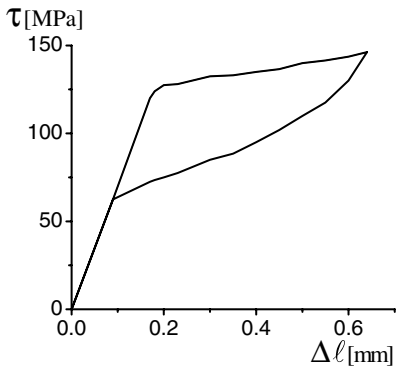

(a)

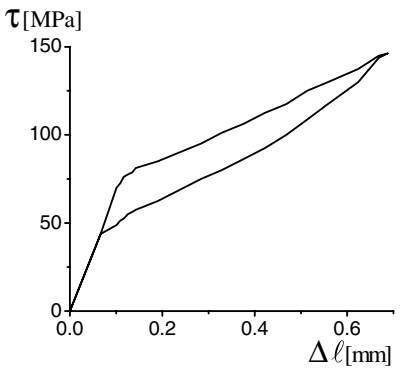

(b)

Fig. 2. (a) Resolved shear stress vs. sample elongation for the first transformation cycle in a specimen with precipitates. Mean volume of precipitates $V = 1.4 \times 10^5\,\mathrm{nm}^3$. (b) Hysteresis loop after 14 cycles. Transformation stresses and hysteresis width strongly decrease with respect to cycle 1 in (a).

(iii) The reverse transformation shows a similar, although not so pronounced, behavior. The stress drop in the reverse transformation stage is roughly 50% of the stress drop in the forward transformation.

(iv) All of the effects mentioned above increase with precipitate volume, considering that the density of precipitates remains constant.

One of the purposes of introducing precipitates is the controlled modification of significant parameters of the alloy. In this sense, it should be remarked that the hysteresis in the asymptotic stage of cycling is an extremely reproducible parameter if γ coherent precipitates are considered. The mean hysteresis, defined as the area enveloped by the cycle loop divided by the elongation due to the transformation, was recorded after 200 cycles for different precipitate sizes.

The results are plotted in Fig. 3, where $\Delta\tau$ is the mean hysteresis width measured in resolved shear stress. A quite linear behavior can be observed, with a slope $\alpha = (187 \pm 5)\,\mathrm{Pa/nm}^3$. This slope can be converted into the amount of energy lost in the hysteresis loops. The energy lost per precipitate volume unit and specimen volume unit can be obtained as follows $w^{\mathrm{Exp}} = \alpha\lambda$, where $\lambda \approx 0.2$ is the amount of the macroscopic shear deformation of the martensitic transformation.[48] The following value is obtained: $w^{\mathrm{Exp}} = (3.7 \pm 0.1) \times 10^{28}\,\mathrm{J/m}^6$.

The origin of the hysteresis can be attributed to the plastic accommodation around the non-transforming precipitates because of the matrix shape change upon transformation. Two stages have been considered as cycling through the transformation is performed.[41,45,49] The first one is associated with the creation of the defects needed to carry the plastic flow. The required stress is considerably greater if precipitates are coherent and dislocations are to be formed around them. This mechanism is active mainly in the first few cycles, producing a marked decrease in hysteresis. In the

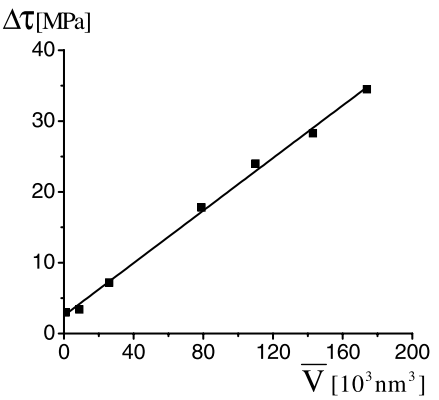

Fig. 3. Asymptotic hysteresis width as a function of average precipitate volume.

second stage, the defects are already present and the plastic deformation around the precipitates takes place in one sense during the β-18R transformation and in the opposite sense during retransformation, leading to asymptotic hysteresis.

A simple model was developed to explain the behavior shown in Fig. 3. The theory of plasticity has been used[41,45] to estimate the irreversible work associated with the transformation. The total (theoretical) work per specimen and precipitates volume unit lost in a closed cycle was found to be

$$w^T \approx 2\tau_c\delta, \tag{1}$$

where τ_c is the critical shear stress to produce the plastic deformation in an ideal, isotropic material. It is possible to attribute internal plastic deformation to several mechanisms (dislocations in β or/in 18R martensite, nucleation and growth of second martensite variants or even martensite to martensite transitions, like 18R–2H or 18R–6R). If an average critical shear stress is used, the following value is obtained: $w^T = (6 \pm 3) \times 10^{28}$ J/m^6,[45] which is in reasonable agreement with the experimental value obtained above. It is then possible to control the asymptotic hysteresis by controlling the precipitation size in the β phase.

It is also interesting to present a short comment on $\Delta\tau$ during the first stage of cycling. This stage is characterized by a rapid decrease in critical transformation stresses and hystereses. In fact, in devices for dissipation of energy during natural events, the first cycles might play a significant role. It is remarkable that the hysteresis drop in the first stage of cycling also depends on the mean precipitate size.[49] Three different regimes have been reported, depending on the precipitate size: in the first regime, the hysteresis drop decreases with precipitate size up to 15 nm size; in the second regime, the hysteresis drop increases with precipitate size up to approximately 30 nm, and, in the third regime, the hysteresis drop increases with a greater slope for larger precipitates, which then become semicoherent.[49] The generation of dislocations was proposed as the explanation of the first two regimes, whereas the presence of microplates of martensite variants was reported in the third regime. Considering the decrease of hysteresis before reaching the asymptotic stage of pseudoelastic cycling, coherent precipitates seem to be a better alternative if larger hystereses are desired.

Finally, it is noticed that the β-18R phase transformation is responsible for the TWSME in CuZnAl alloys, a phenomenon which is also affected by the presence of γ precipitates in the matrix.[50,51] The TWSME has attracted much attention in the frame of SMAs because it is not an intrinsic property but can be introduced by a specific training method. This effect is characterized by a shape change taking place during both thermally induced martensitic transformations: austenite to martensite and the retransformation to austenite. The shape change obtained during heating is readily explained by the movement of the atoms to their original sites in the austenite. However, the shape change obtained during cooling requires some anisotropy among the martensite variants, which usually requires the modification of the microstructure.[52–55] In Cu-based alloys the deformation of the material is minimized while the thermally induced martensitic transformation takes place, leading to the nucleation and growth of several martensite variants, which compensate individual shape changes. It is, then, necessary to favor a selected amount of variants, preferably only one, to obtain the maximum shape change during cooling. This is the goal of scientists working on this phenomenon.

Several thermomechanical treatments have been reported as suitable methods to introduce the TWSME in Cu–Zn–Al alloys. As typical examples, we can mention thermal cycling under applied stress and pseudoelastic cycling at constant temperature. The introduction of precipitates has been shown to have several effects concerning the TWSME. These effects might be classified according to two contradictory consequences: on the one hand, it has been shown that the introduction of precipitates favor the generation of the shape change during cooling[56–58] but, on the other hand, they might contribute to the degradation of the desired phenomenon.[50,59]

This degradation can be related to the presence of equilibrium precipitates which decrease the amount of β phase available for the transformation. As a consequence of this effect, the improvement of the TWSME by the introduction of coherent γ precipitates is more attractive. We mention a couple of examples of this positive influence:

(i) The number of pseudoelastic cycles required to induce the TWSME is strongly reduced by the presence of γ nanoprecipitates, while the amount of cycles to introduce dislocation arrays increases.[56] This was explained by a hardening effect of the martensite in addition to the symmetry around precipitates which is broken due to dislocations loops observed surrounding the small particles.

(ii) Large strain fields were reported by Zhang *et al.* around precipitates which are spherical in martensite but show an ellipsoidal shape in β. These precipitates were introduced during the training method.[60]

(iii) Isalgué *et al.* have shown that no training is required if anisotropic introduction of precipitates is performed.[57] These precipitates were grown in the β matrix under compressive stress, which changed their shape from cuboidal to ellipsoidal. The main point here is that the introduction of this anisotropy was enough to induce the TWSME, which is probably related to residual stresses, whose origins are both elastic and plastic.

3. The Effect of Precipitates on the 18R–6R Martensitic Transition in CuZnAl Alloys

One of the main characteristics of the 18R–6R martensitic transition in CuZnAl alloys is its huge hysteresis, which makes it a potential candidate for mechanical damping devices. However, for the alloy compositions used in this work, the 18R–6R martensitic transformation is different from the beta-18R transformation in several ways. Firstly, it is not possible to induce the 18R–6R transformation by temperature changes, it can only be induced by tension stress, whereas the β-18R transformation can be easily induced by temperature changes or by mechanical stresses (tension or compression). Secondly, the 18R–6R transformation can only be induced in crystals with specific crystallographic orientations, i.e., close to [1 0 0]. This happens because the 18R–6R transformation stress is relatively close to the fracture stress of the brittle 18R phase. If the crystallographic orientation of the single crystal is not favorable to the 18R–6R transformation, brittle fracture of the 18R phase will occur before the formation of 6R. The need for a favorable crystallographic orientation for the 18R–6R transformation to take place is what prevents the formation of 6R in polycrystalline samples with random crystallographic orientation. However, it should be possible to have 18R–6R transformation in polycrystalline samples with adequate crystallographic texture and/or unconventional structures, as has been reported in CuAlNi.[61]

Moreover, the 18R–6R transition stress is less sensitive to temperature variations than the β-18R transition, i.e., the modulus of the Clausius–Clapeyron coefficient of the 18R–6R transition is smaller than the modulus of the Clausius–Clapeyron coefficient of the β-18R transition.[4,62] Interestingly, some studies have reported that the Clausius–Clapeyron coefficient of the 18R–6R transition is smaller than zero, which means that the transition stresses should decrease as temperature increases.

A significant limitation of the 18R–6R transformation in CuZnAl is that, at $e/a = 1.48$, the 18R–6R transition occurs simultaneously with the plastic deformation of the 6R phase.[7,63] The plastic deformation of the 6R martensite immediately after its formation from the 18R phase is unfortunate, as it interferes with the pseudoelastic effect and prevents the alloy from completely recovering its original shape once the load is removed. In other words, complete shape recovery is not achieved because of the plastic deformation of the 6R phase. Moreover, it is not easy, if at all possible, to obtain a value for the plastic deformation stress of the 6R phase, but it is reasonable to state that the yield stress of the 6R phase is below the 18R–6R transformation stress, so the 6R deforms plastically immediately after its formation. This plastic deformation, in turn, increases the stress required for further plastic deformation until it is equal to the 18R–6R transformation stress. In other words, the recently formed 6R phase undergoes work hardening until the local flow stress is equal to its transformation stress. This phenomenon might explain the jerky behavior of the 18R–6R transformation when no precipitates are present.

Two different approaches have been proposed to prevent the plastic deformation of the 6R martensite. The first approach is the modification of the chemical composition of the alloy so as to reduce the e/a ratio to 1.43 or below. The reduction of the e/a ratio effectively lowers the 18R–6R transition stress, making it possible to obtain 6R martensite without plastic deformation.[63] However, two significant side effects are introduced by this approach. On the one hand, the fatigue life of alloys at $e/a = 1.43$ or below is very low, i.e., fracture occurs after a small number of mechanical cycles.[64] On the other hand, as the e/a ratio distances itself from 1.48, it becomes increasingly difficult to retain the metastable beta phase at room temperature without decomposition into other phases. This happens because the lowest temperature at which the beta phase is stable occurs at $e/a = 1.48$. In other words, we can say that the e/a that corresponds to the highest stability of the β phase in CuZnAl is 1.48 and, as the e/a ratio decreases — or increases, for that matter — it becomes increasingly more difficult to manufacture the alloy. Once the alloy solidifies, it must be quickly cooled, i.e., quenched to room temperature, otherwise, the metastable phase decomposes into the stable alpha and gamma phases. The same reasoning applies to high temperature thermal treatments, e.g., to solubilize precipitates. After the thermal treatment, the alloy must be quickly quenched to avoid the decomposition of the beta phase. It is important to emphasize that even at $e/a = 1.48$ the beta phase is metastable at room temperature. Having a metastable austenitic phase is a necessary condition for martensitic transformations, as a stable phase will not undergo a martensitic transformation.

The other possible approach to obtain 6R without simultaneous plastic deformation in CuZnAl alloys is to induce a distribution of gamma phase precipitates with a controlled thermal treatment. The obvious advantage of this approach is that alloys with $e/a = 1.48$ can be used. These alloys are easier to manufacture and have longer fatigue lives than alloys with lower e/a ratios. Precipitates pin dislocations (Orowan effect), effectively increasing the plastic deformation stresses. However, precipitates also act as barriers to martensitic transformation fronts, interfering with their movement. This phenomenon increases the 18R–6R transformation stress, so it is not immediately obvious whether precipitates can effectively allow the formation of 6R without plastic deformation. In order to be effective, the increase in the plastic deformation stress of the 6R phase must be significantly greater than the increase in the 18R–6R

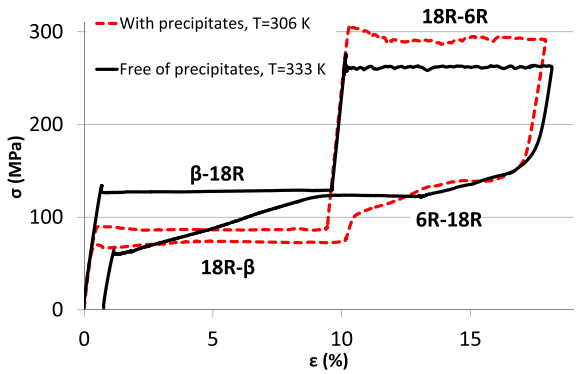

Fig. 4. The effect of precipitates on the mechanical behavior of CuZnAl single crystals with $e/a = 1.48$. Without precipitates, significant permanent deformation is observed once the load is removed (black solid line). With precipitates, no permanent deformation is observed (red pointed line).

transformation stress. Precipitates also modify the chemical composition of the matrix. Specifically, γ phase precipitates are rich in Al so their formation tends to decrease the e/a ratio of the matrix.[65] However, as the total fraction of small precipitates grown with the thermal treatments described in this paper is small, the reduction in e/a caused by precipitation is small. When two CuZnAl single crystals ($e/a = 1.48$, the same crystallographic orientation and the same chemical composition), one with precipitates and the other free of precipitates, are submitted to a tension test until the 18R–6R formation, the difference in mechanical behavior caused by the precipitates is very clear (Fig. 4).

A specific study was carried out to verify the possibility of obtaining 6R without plastic deformation by introducing a distribution of nanometric precipitates in the alloy.[66] The step-quench thermal treatment used was selected because it produces a distribution where the distance between precipitates is minimized. Being closer to each other, precipitates are more effective in pinning dislocations, which results in a greater increase in plastic deformation stress. Results show that, with precipitates, it is possible to obtain 6R without plastic deformation. When the load is removed, the sample returns to its original length. No permanent deformation is observed. Thus, we can conclude that the increase in the plastic deformation stress caused by precipitates is greater than the increase in the 18R–6R transformation stress.

Precipitates have also proven to be effective in preventing plastic deformation during 18R–6R mechanical cycling, especially at higher frequencies.[35] More research on the metallurgical phenomena that lead to the effects observed is required, but the introduction of an optimized distribution of γ-phase precipitates is a relatively simple approach to improving the mechanical reversibility of the 18R–6R transition in CuZnAl alloys.

4. Conclusions

Precipitates have a very strong effect on the properties of CnZnAl SMAs, which means that they are an effective engineering tool to modify the mechanical behavior of these alloys. With adequate thermomechanical processing, the β-18R and 18R–6R hystereses can be tuned to desired values. Moreover, some behaviors which are not intrinsic to these alloys can be observed with specific distributions of precipitates: the TWSME and the 18R–6R transformation without plastic deformation in CuZnAl with $e/a = 1.48$.

Acknowledgments

This work has been supported by CNEA, ANPCyT Argentina (PICT 2012-0884), CONICET (PIP 0513) and U. N. Cuyo (06/C482).

References

1. T. Maki and I. Tamura, Shape memory effect in ferrous alloys, *Proc. ICOMAT* (1986), pp. 963–970.
2. K. Otsuka and C. M. Wayman, *Mechanism of Shape Memory Effect and Superelasticity*, eds. K. Otsuka and C. M. Wayman, Chap. 2 (Cambridge University Press, Cambridge, 1998), pp. 27–48.
3. J. Van Humbeeck and R. Stalmans, *Characteristics of Shape Memory Alloys*, eds. K. Otsuka and C. M. Wayman, Chap. 7 (Cambridge University Press, Cambridge, 1998), pp. 149–183.
4. M. Ahlers, *Prog. Mater. Sci.* **30**, 135 (1986).
5. V. Novák, P. Sittner, D. Vokun and N. Zárubová, *Mater. Sci. Eng. A* **273–275**, 280 (1999).
6. A. Yawny, F. C. Lovey and M. Sade, *Mat. Sci. Eng. A* **290**, 108 (2000).
7. G. Barceló, M. Ahlers and R. Rapacioli, *Z. Metallkd* **70**, 732 (1979).
8. K. Otsuka, H. Sakamoto and K. Shimizu, *Acta Metall.* **27**, 585 (1979).
9. F. de Castro Bubani, M. Sade, V. Torra, F. Lovey and A. Yawny, *Mat. Sci. Eng. A* **583**, 129 (2013).
10. M. Sade, P. La Roca, F. De Castro Bubani, F. C. Lovey, V. Torra and A. Yawny, *Mater. Today Proc.* **2S**, S719 (2015).
11. V. Torra, A. Isalgue, F. Martorell, P. Terriault and F. C. Lovey, *Eng. Struct.* **29**, 1889 (2007).
12. S. A. Motaharia, M. Ghassemieha and S. A. Abolmaalib, *J. Constr. Steel Res.* **63**, 1570 (2007).
13. M. Dolce and D. Cardone, *Int. J. Mech. Sci.* **43**, 2631 (2001).
14. M. Dolce and D. Cardone, *Int. J. Mech. Sci.* **43**, 2657 (2001).
15. G. Song, N. Ma and H. N. Li, *Eng. Struct.* **28**, 1266 (2006).
16. T. Saburi, *Ti–Ni Shape Memory Alloys*, eds. K. Otsuka and C. M. Wayman, Chap. 3 (Cambridge University Press, Cambridge, 1998), pp. 49–96.
17. N. Zhou, C. Shen, M. F. X. Wagner, G. Eggeler, M. J. Mills and Y. Wang, *Acta Mater.* **58**, 6685 (2010).
18. Yawny, M. Sade and G. Eggeler, *Z. Metallkd.* **96**, 608 (2005).
19. A. Baruj, T. Kikuchi, S. Kajiwara and N. Shinya, *Mater. Sci. Eng. A* **378**, 333 (2004).

20. T. Omori, K. Ando, M. Okano, X. Xu, Y. Tanaka, I. Ohnuma, R. Kainuma and K. Ishida, *Science* **333**, 68 (2011).
21. Y. Tanaka, Y. Himuro, R. Kainuma, Y. Sutou, T. Omori and K. Ishida, *Science* **327**, 1488 (2010).
22. I. V. Kireeva, C. Picornell, J. Pons, I. V. Kretinina, Yu. I. Chumlyakov and E. Cesari, *Acta Mater.* **68**, 127 (2014).
23. M. Sade, R. Rapacioli and M. Ahlers, *Acta Metall.* **33**, 467 (1985).
24. A. Tolley, D. Ríos Jara and F. C. Lovey, *Acta Metall.* **37**, 1099 (1989).
25. R. Gastien, C. E. Corbellani, M. Sade and F. Lovey, *Acta Mater.* **53**, 1685 (2005).
26. M. Sade, J. L. Pelegrina, A. Yawny and F. C. Lovey, *J. Alloys Compd.* **622**, 309 (2015).
27. M. L. Castro and R. Romero, *Mater. Sci. Eng. A* **255**, 1 (1998).
28. M. L. Castro and R. Romero, *Mater. Sci. Eng. A* **273–275**, 577 (1999).
29. S. Montecinos, A. Cuniberti and R. Romero, *Intermetallics* **19**, 35 (2011).
30. H. Warlimont and L. Delaey, *Martensitic Transformations in Copper-Silver and Gold-based Alloys*, Progress in Material Science, Vol. 18, eds. B. Chalmers, J. W. Chtistian, T. B. Massalski (Pergamon Press, 1974).
31. J. L. Pelegrina and M. Ahlers, *Acta Metall. Mater.* **40**, 3205 (1992).
32. A. Cuniberti, R. Romero and A. Condó, *Mater. Sci. Eng. A* **325**, 177 (2002).
33. N. Zárubová, A. Gemperle and V. Novák, *Mater. Sci. Eng. A* **222**, 166 (1997).
34. V. E. A. Araujo, R. Gastien, E. Zelaya, J. I. Beiroa, I. Corro, M. Sade and F. C. Lovey, *J. Alloys Compd.* **41**, 155 (2015).
35. F. De Castro Bubani, M. Sade and F. Lovey, *Mater. Sci. Eng. A* **557**, 147 (2013).
36. R. Rapacioli and M. Chandrasekaran, The influence of thermal treatments on martensitic transformation in Cu–Zn–Al, *Proc. ICOMAT* (1979), pp. 596–601.
37. C. Auguet, E. Cesari, R. Rapacioli and Ll. Mañosa, *Scr. Metall.* **23**, 579 (1989).
38. F. C. Lovey and E. Cesari, *Mater. Sci. Eng. A* **129**, 127 (1990).
39. J. Pons and E. Cesari, *Thermochim. Acta* **145**, 237 (1989).
40. J. Pons, E. Cesari and M. Roca, *Mater. Lett.* **9**, 542 (1990).
41. F. C. Lovey, V. Torra, A. Isalgue, D. Roqueta and M. Sade, *Acta Metall. Mater.* **42**, 453 (1994).
42. F. C. Lovey and V. Torra, *Prog. Mater. Sci.* **44**, 189 (1999).
43. J. Van Humbeeck, *Mater. Sci. Eng. A* **273–275**, 134 (1999).
44. T. Duerig, A. Pelton and D. Stockel, *Mater. Sci. Eng. A* **273–275**, 149 (1999).
45. D. Roqueta, F. C. Lovey and M. Sade, *Scr. Metall.* **34**, 1747 (1996).
46. J. Pons and R. Portier, *Acta Mater.* **45**, 2109 (1997).
47. R. Rapacioli, M. Chandrasekaran and F. C. Lovey, Precipitation in βCu–Zn–Al, *Proc. Int. Conf. on Solid — Solid Phase Transformations* (1981), pp. 739–743.
48. J. De Vos, E. Aernoudt and L. Delaey, *Z. Metallkd* **69**, 438 (1978).
49. D. O. Roqueta, F. C. Lovey and M. Sade, *Scr. Mater.* **36**, 385 (1997).
50. L. Contardo, P. Naudof and G. Guénin, Stability and ageing of the two way shape memory effect in a Cu–Zn–Al alloy, *Proc. ESOMAT* (1988), pp. 157–164.
51. L. Contarto and G. Guénin, *Acta Metall. Mater.* **38**, 1267 (1990).
52. E. Cingolani, M. Ahlers and M. Sade, *Acta Metall. Mater.* **43**, 2451 (1995).
53. E. Cingolani and M. Ahlers, *Mater. Sci. Eng. A* **273–275**, 595 (1999).
54. C. Picornell, R. Rapacioli, J. Pons and E. Cesari, *Mater. Sci. Eng. A* **273–275**, 605 (1999).
55. J. Malarría, F. C. Lovey and M. Sade, *Mater. Sci. Eng. A* **517**, 118 (2009).
56. J. Pons, M. Sade, F. C. Lovey and E. Cesari, *Mater. Trans. JIM* **34**, 888 (1993).
57. A. Isalgué, F. C. Lovey and M. Sade, *Scr. Meter.* **28**, 1183 (1993).
58. X. M. Zhang, J. M. Guilemany, J. Fernandez, M. Liu and L. Liu, *Intermetallics* **8**, 703 (2000).
59. S. Datta, A. Bhunya and M. K. Banerjee, *Mater. Sci. Eng. A* **300**, 291 (2001).
60. X. M. Zhang, M. Liu, J. Fenandez and J. M. Guilemany, *Mater. Des.* **21**, 557 (2000).
61. H. Fu, S. Song, L. Zhuo, Z. Zhang and J. Xie, *Mater. Sci. Eng. A* **650**, 218 (2016).
62. M. Ahlers and J. L. Pelegrina, *Acta Metall. Mater.* **40**, 3213 (1992).
63. A. Cuniberti and R. Romero, *Mater. Sci. Eng. A* **273–275**, 362 (1999).
64. C. Damiani and M. Sade, *Mater. Sci. Eng. A* **273–275**, 616 (1999).
65. D. O. Roqueta, F. C. Lovey and M. Sade, *Scr. Mater.* **40**, 1359 (1999).
66. F. C. Bubani, M. Sade and F. Lovey, *Mater. Sci. Eng. A* **543**, 88 (2012).